PSEUDO-DYNAMIC MODEL OF A BIO-ETHANOL PROCESSOR FOR A FUEL CELL HYBRID VEHICLE

Lucas Nieto Degliuomini[(a)], David Zumoffen[(a)], Diego Feroldi[(a)], Marta Basualdo[(a)], Rachid Outbib[(b)]

[(a)] CIFASIS-CONICET, Bv 27 de Febrero 210 bis, Rosario, Argentina.
[(b)] LSIS, Université Paul Cézanne Aix-Marseille, France.

[(a)] nieto,zumoffen,feroldi,basualdo@cifasis-conicet.gov.ar, [(b)] rachid.outbib@lsis.org

ABSTRACT

The transient behavior of a Fuel Processor System to produce Hydrogen from bio-ethanol with high performance, coupled with a Proton Exchange Membrane Fuel Cell is modeled. The Ethanol Processor is based on a previous steady state design, optimized to work with maximum efficiency around 10 kW of rated power. The Fuel Cell System is then hybridized with supercapacitors as auxiliary power source, to lower the overall consumption of hydrogen, hence of bio-ethanol too. The entire vehicle is tested using standard driving cycles, widely utilized in related literature and to measure pollutant emissions. The overall behavior reaches the expectations and is capable of fulfilling the requirements of urban and highway scenarios, and also suggests the possibility of resizing the components to improve fuel economy.

Keywords: Fuel Cell Hybrid Vehicles, Energy Management Strategies, Bio-ethanol Fuel Processor

1. INTRODUCTION

Fuel Cell Hybrid Vehicles (FCHV) is a promising application of fuel cell technology that has taken more and more importance in the last years and is considered the most attractive long-term option for passenger cars. Hybridization in FCHV consists in adding a supplementary energy storage element (e.g., a battery or an supercapacitor (SC) bank) to the primary power source, i.e. Proton Exchange Membrane Fuel Cell (PEMFC), in order to adequate optimally the energy generation to the consumption with almost zero emission. PEMFC are devices that convert chemical energy in the form of hydrogen into electricity with high efficiency, without passing through a combustion stage. Hybridization has important advantages, allowing a greater reduction of the hydrogen consumption, and its economical importance has been recently remarked in (Offer et al. 2010).

Validated mathematical models provide a powerful tool for the development and improvement of the fuel cell technology. Mathematical models can be used to describe the fundamental phenomena that take place in the system to predict the behavior under different operating conditions and to design and optimize the control of such complex systems. In this work, a complete model of a FCHV powered by a hybrid system composed by a PEM fuel cell and a supercapacitor bank is done. Besides, the PEM fuel cell is fed with hydrogen from a bio-ethanol processor, which is also modeled. Finally, the complete model is integrated with an Energy Management Strategy, which is in charge of properly managing the PEM fuel cell to supply the power requirements of the vehicle to fulfill the testing profiles. Some works have appeared regarding to the power management of hybrid vehicles with multiple energy sources, such as fuel cell, battery and supercapacitor (Thounthong et al. 2009, Li et al. 2009). The management strategy used in this work, developed by (Feroldi et al. 2009), is described in Section 3.

A preliminary plant-wide control structure for the process of producing hydrogen from bio-ethanol to be used in a PEM fuel cell has been presented in (Biset et al. 2009). This control structure accounts only steady-state information. In this work, the operational conditions for the PEMFC were adopted from recommendations given by (Pukrushpan et al. 2004). In this last work, a deep study about control of fuel cell systems, with focus on air-flow control was presented. Hence, believing on the high quality of that work, in this paper is used the same control oriented model of the PEMFC which is considered as a benchmark. In (Pukrushpan et al. 2004), several control strategies are proposed accounting abrupt current demand from the vehicle. They concluded that the air supply must be promptly increased to replenish the cathode with oxygen.

There are few publications regarding fuel processors dynamic behavior, some using methanol as raw material, such as (Chuang et al. 2008), and very recently some publications on using ethanol to produce hydrogen. Some of these are (Aicher et al. 2009, Garcia et al. 2009). Even though they present

dynamic models, or experimental results, and use them to synthesize control structures, they do not contemplate the energy integration, and the combination of the Fuel Cell System with energy storage devices, which makes this technology economically feasible and highly interacted. The research works previously mentioned highlighted the main difficulties and objectives to account in the operation of fuel processors and fuel cell systems, which are vital to assure the catalysts working life and to avoid damage to the components. This is the first work that deals with the entire hybrid vehicle integrated, meaning Fuel Processor Plant, Fuel Cell System, Energy Storage System, Energy Management Strategy and Powertrain models, and it is rigourously tested using standardized driving cycles.

The structure of the paper is as follows: in Section 2, the complete model of the system is described, while in Section 3 the model is integrated with an Energy Management Strategy. In Section 4, the model is validated through simulation using Standard Driving Cycles widely used in the literature. Finally, application results and conclusions are provided in Section 5 and 6, respectively.

2. DESCRIPTION OF THE MODEL

The model presented en this work consists of the following submodels: Fuel Processor model, PEM Fuel Cell model, Energy Storage System model and vehicle model.

2.1 Fuel Processor model

The Fuel Processor System (FPS) (illustrated in Fig. 1) consists of a Bio-Ethanol Steam Reforming (ESR) plug flow reactor, where most of the conversion of bio-ethanol to H_2 is made. Since carbon monoxide (CO), which poisons the fuel cell catalyst, is produced in the ESR, additional processing is needed to remove this substance. There are three reactors that configure the cleaning system. These are two Water Gas Shift (WGS), one of high temperature (fast) and the other of low temperature, that favors the equilibrium of the reaction to higher conversion rates of CO. The third is a Preferential Oxidation of Carbon monoxide (CO-PrOx) reactor, where oxidation of CO into CO_2 is made. Also, the undesired oxidation of H_2 occurs. Therefore, the catalyst is selected to improve the conversion of CO.

Ethanol and vaporized water are mixed and then supplied to the ESR reactor, to produce ethanol decomposition:

$$\text{(ESR)} \quad CH_3CH_2OH + 3H_2O \leftrightarrow 6H_2 + 2CO_2 \quad (1)$$

The overall reaction is endothermic, and heat requirement is supplied by a burner, which is fed with ethanol and compressed air. The transfer of heat is achieved passing the hot gases through the jacket of the reformer. The produced reaction inside the WGS is:

$$\text{(WGS)} \quad CO + H_2O \leftrightarrow CO_2 + H_2 \quad (2)$$

This reaction produces heat and creates more hydrogen. Levels of CO are still high even after the two WGS reactors. Therefore the final elimination is made in the CO-PrOx reactor, which produces the oxidation of CO. The WGS reaction takes place in this reactor too. Oxygen is injected into the CO-PrOx, the amount needed is about twice the stoichiometric relation to have a good selectivity and satisfy the requirements of the FC.

The plug flow reactors are modeled as 20 lined-up Continuous Stirred Tank Reactors (CSTR). The molar flow between two volumes is given by the orifice flow equation as a function of upstream pressure, and downstream pressure. Further details on the dynamic modeling, process constraints and normal behavior can be seen in (Nieto et al. 2009).

2.2 Proton Exchange Membrane Fuel Cell

Fuel cells convert chemical energy directly into electrical energy. They are constituted by an anode, where H_2 is injected, and a cathode, where the oxidant, normally air is injected. The electrodes are separated by a membrane that allows the proton exchange and contribute to the oxidation reaction to produce electrical power. The cell generates an open-circuit voltage which is affected by a number of losses (activation, concentration and ohmic) that leads to a useful actual voltage. (Pukrushpan et al. 2004) presents a rigorous dynamic model of a PEMFC which is used in this work. In this work, the model has been adapted to represent a PEM fuel cell model with a maximum power of 10 kilowatts. Transient behavior of manifold filling, membrane hydration, the air compressor and the heat management are included in the model. Interaction between processes are also included.

2.3 Energy Storage System model

The energy storage system, either if it is based on batteries or supercapacitors, can be modelled with two subsystems. One subsystem takes into account the system efficiency, both during charging and discharging, and the other subsystem computes the actual energy level. The energy stored in the storage system, $E_{ess}(t)$, results integrating $P_{ess}(t)$:

$$E_{ess}(t) = E_{ess}(0) + \int_0^{t_c} P_{ess}(t)dt. \quad (3)$$

It is useful to define a parameter that indicates the relative amount of energy in the *ESS*. The *State of Energy*, *SoE(t)*, is defined as

$$SoE(t) = \frac{E_{ess}(t)}{E_{cap}} \times 100 \qquad [\%], \quad (4)$$

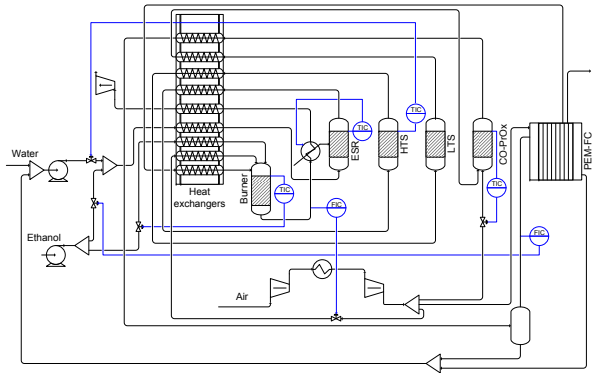

Figure 1: Complete prototype with control structure

where E_{cap} is the maximum energy that the storage system is capable to store.

The *ESS* efficiency, in this case a supercapacitor bank, is related with the equivalent series resistance (*ESR*). For a pure capacitor, having zero *ESR*, the efficiency of charge or discharge would be 100%. However, in a real capacitor, having nonzero *ESR*, the irreversible dissipation of power is $ESR \cdot I_{sc}^2$, giving efficiencies lower than 100%. The equivalent parallel resistance (*EPR*) represents the self-discharge losses and only impacts long-term energy storage performance of the *SC* and is extremely high (Uzunoglu et al. 2007). Thus, the time constant of the period of charge/discharge can be expressed by $ESR \cdot C$. Since *ESR* is as low as 0.019Ω and C is 58 F, it is possible to charge and discharge the *SC* in a very short time. The energy stored in the *SC* is directly proportional to the capacitance and the squared voltage.

2.4 Vehicle model

In order to integrate the Fuel Processor model and the Fuel Cell System model with an entire vehicle and the energy management strategy, a detailed vehicle model has been developed in ADVISOR, a MATLAB toolbox developed by the National Renewable Energy Laboratory with the aim of analyzing the performance and fuel economy of conventional, electric, and hybrid vehicles (Markel et al. 2002). The fuel cell model, the fuel processor model, the energy storage model, and the energy management strategy discussed in section 3 are integrated to form a complete model representing the FCHV with on-board bio-ethanol reforming. The integrated power train along with the energy flows is shown in Fig. 2.

In this work, we consider the performance of a FCHV based on a small car and the entire system being modelled in *ADVISOR* according with the principal parameters listed in Table 1.

Table 1: Vehicle specifications in the case of study.

Specification	Symbol	Value	Unit
Vehicle total mass	m_T	1380	kg
Vehicle mass[a]	m_{veh}	882	kg
Frontal area	A_f	2	m^2
Drag coefficient	C_d	0.335	-
Coefficient of rolling friction	f_r	0.009	-
Air density	ρ_a	1.2	$kg\,m^{-3}$
Gravity	g	9.8	$m\,s^{-2}$

[a] Vehicle mass without taking into account the *FCS* mass and the *ESS* mass.

2.5 Computational Model Implementation

The pressure requirements are satisfied in stationary state with compressors and turbines modeled in HYSYS (Aspen 2006). It supports the important data bank information for the different components. In addition, the LNG tool in HYSYS, that solves material and heat balances for multi-stream exchangers and heat exchangers networks. On the other hand, the dynamic model of the reactors is developed in MATLAB, which integrates the differential equations. The communication interface is performed by the use of the spreadsheets in HYSYS and a specific library for doing the corresponding data transference and updating at scheduled sampling time between both programs. Since the components in HYSYS are considered in steady state, and the reactors set in MATLAB are modeled dynamically, the communication protocol is required to coordinate the calculations. The dynamic behavior of the FPS is considerably slower than the auxiliary components, so this last one is neglected, considered in a pseudo-dynamic way. The frequency of update is fixed in 0.05 seconds of simulation time, in order to capture the fastest dynamics of the chemical reactions taking place

2.5.1 Heat Integration

The heat integration in the model is performed by the LNG tool working in a pseudo-dynamic mode. It is called by MATLAB for determining the instantaneous temperature values of the different cold and hot streams of the process. Therefore, it is assumed that the dynamic effect of the heat exchangers network is neglected. The minimum heat requirement of the system and the minimum heat to be evacuated can be computed for each operating point or with the system under different disturbances.

3. INTEGRATION OF THE MODEL WITH THE ENERGY MANAGEMENT STRATEGY

The management strategy used in this work is based on the fuel cell efficiency map and it operates the fuel cell preferably in its point of maximum effi-

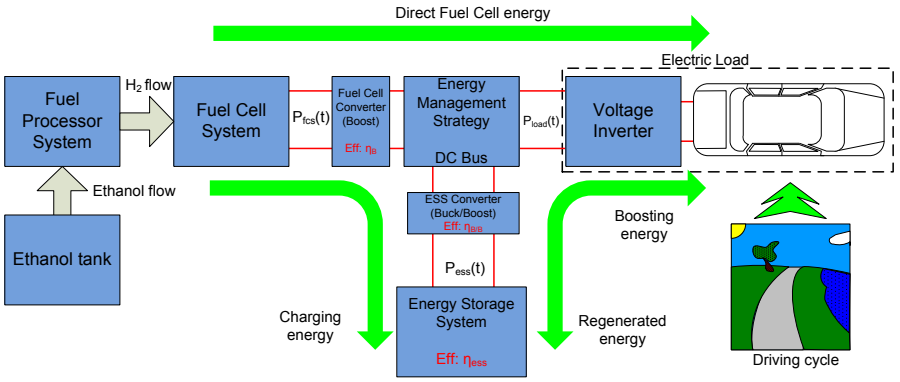

Figure 2: Configuration of the FCHV model with on-board bio-ethanol reforming

ciency in order to improve the hydrogen economy, although the final operating point of the fuel cell is determined based on the actual power demand and the state of energy (SoE) of the Energy Storage System (ESS) (Feroldi 2009).

The fuel cell power command is determined according to the following rules (the nomenclature is explained in Table 2). If the load power is

$$P_{fcs,lo} \cdot \eta_B \leq P_{load}(k) \leq P_{fcs,hi} \cdot \eta_B \tag{5}$$

and, the SoE is

$$SoE_{lo} \leq SoE(k) \leq SoE_{hi} \tag{6}$$

where $P_{fcs,hi}$ is

$$P_{fcs,hi} = P_{fcs,max} \cdot \eta_B \cdot X_{fcs,hi} \tag{7}$$

and $X_{fcs,hi}$ is a fraction of the maximum FCS power; then, the FCS is operated in its point of maximum efficiency (Zone 2 in Fig. 3)

$$P_{fcs}(k) = P_{fcs,maxeff} \tag{8}$$

The remaining power to achieve the load demand flows from or to the ESS according to

$$P_{ess}(k) = \min \left\{ \begin{array}{c} \frac{(P_{load}(k) - P_{fcs}(k) \cdot \eta_B)}{\eta_{B/B} \cdot \eta_{ess}} \\ (SoE(k) - SoE_{min})\, k_{ess} \end{array} \right\} \tag{9}$$

if $P_{load}(k) > P_{fcs,maxeff}$ (discharging mode), or

$$P_{ess}(k) = -\min \left\{ \begin{array}{c} \mid P_{load}(k) - P_{fcs}(k)\, \eta_B \mid \eta_{ess} \eta_{B/B} \\ \mid SoE(k) - SoE_{max} \mid k_{ess} \end{array} \right\} \tag{10}$$

if $P_{load}(k) < P_{fcs,maxeff}$ (charging mode).

If the load power is

$$P_{fcs,hi} \cdot \eta_B \leq P_{load}(k) \leq P_{fcs,max} \cdot \eta_B \tag{11}$$

and, the SoE is

$$SoE_{lo} \leq SoE(k) \leq SoE_{hi} \tag{12}$$

Table 2: Nomenclature utilized

Symbol	Description	Value
k	Current time	Seconds
$P_{fcs,lo}$	Lower net power	4000 W
$P_{fcs,hi}$	Higher net power	8000 W
P_{load}	Demanded Power	W
P_{fcs}	FC net power	W
P_{ess}	ESS output power	W
$P_{fcs,max}$	Maximum net power	10000 W
$P_{fcs,maxeff}$	Maximum efficiency net power	8000 W
η_B	FC converter efficiency	0.95
$\eta_{B/B}$	ESS converter efficiency	0.95
η_{ess}	ESS efficiency	0.95
SoE_{lo}	Lower SoE	0.4
SoE_{hi}	Higher SoE	0.8
SoE_{min}	Mimimum SoE	0.3
SoE_{max}	Maximum SoE	0.9
T_{off}	Time to turn off FC	60 sec

then, the FCS is operated in load following mode (Zone 3 in Fig. 3)

$$P_{fcs}(k) = \frac{P_{load}(k)}{\eta_B} \tag{13}$$

and $P_{ess}(k)$ is as indicated in (10) or (9).

On the other hand, if

$$P_{load}(k) \geq P_{fcs,max} \cdot \eta_B \text{ and } SoE(k) \leq SoE_{hi} \tag{14}$$

or

$$SoE(k) \leq SoE_{lo} \tag{15}$$

then, the FCS is operated at its maximum power (Zone 4 in Fig. 3)

$$P_{fcs}(k) = P_{fcs,max} \tag{16}$$

and $P_{ess}(k)$ is as indicated in (9). If, on the contrary

$$P_{load}(k) \leq P_{fcs,lo} \cdot \eta_B \text{ and } SoE(k) \geq SoE_{lo} \tag{17}$$

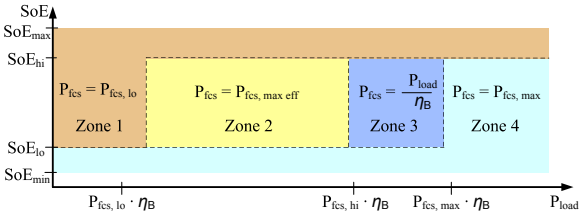

Figure 3: FCS operating point as a function of the SoE and the load power for the strategy based on efficiency map.

or $SoE\,(k) \geq SoE_{hi}$, then, the FCS is working at its lower operating point (Zone 1 in Fig. 3)

$$P_{fcs}\,(k) = P_{fcs,lo} \tag{18}$$

and $P_{ess}\,(k)$ is as in (10). Additionally, if $P_{load}\,(k) = 0\ \forall t \in [k1, k2]$ with $(k2 - k1) > T_{off}$, and, $SoE\,(k) > SoE_{hi}$ with $k > k2$, then, the FCS is turned off to avoid unnecessary hydrogen consumption because the parasitic losses in the FCS. Fig. 3 indicates the FCS operating point as a function of the $SoE\,(k)$ and the load power $P_{load}\,(k)$. The transition between operating points is performed according to the constraints concerning the maximum fall power rate and the maximum power rate.

4. VALIDATION OF THE MODEL

In order to evaluate the performance of a given hybrid vehicle, standard driving cycles are widely utilized in the literature. They represent urban and highway scenarios and were originally stated for measuring pollutant emissions and fuel economy of engines (DieselNet 2010).

In the driving cycles high power requirements take place during a relatively short fraction of time. If there is no energy storage, the FCS must meet the highest peak power and, therefore, the FCS is oversized most of the time. In addition, the efficiency of a FCS is strongly degraded at low powers. Thus, if no hybridization is present, the FCS has to work in large periods of time at a low efficiency zone.

On the contrary, with an additional power source and a suitable energy management strategy it is possible to avoid these unfavorable operating zones. In a fuel cell hybrid system it is possible to boost the FCS supplying energy to the load from the energy storage system. This energy was previously charged from the FCS or regenerated from the load, e.g., from regenerative braking in automotive applications.

5. APPLICATION RESULTS

The FCHV with on-board bio-ethanol reforming is tested using four standardized driving cycles: the New European Driving Cycle (NEDC), the Urban Dynamometer Driving Schedule (UDDS), the Federal Test Procedure (FTP), and the Highway Fuel Economy Cycle (HWFET). The results corresponding to the NEDC and the UDDS are shown in Figs. 4 and 5, respectively. For each group of figures, the speed requirements; power split between the FC and storage system; O_2 excess ratio in the cathode; working zone, and H_2 production are plotted. It can be seen that both the management strategy and the FCS are capable of working properly against the wide range of power demands proposed by the driving cycles.

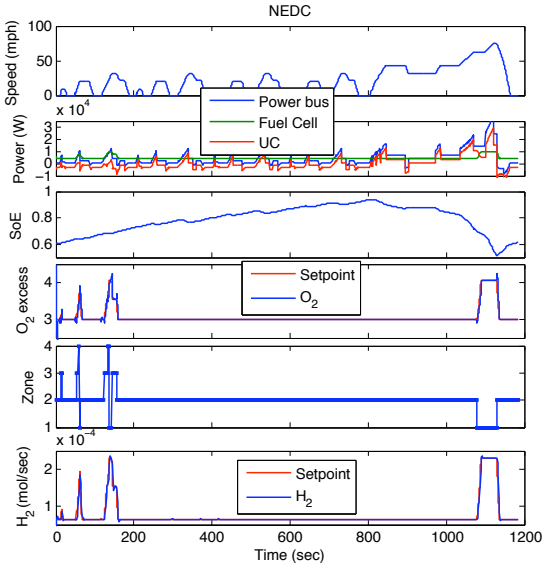

Figure 4: Simulation results for NEDC.

In Fig. 6, an evaluation of the bio-ethanol consumption is done, for the four cycles in study. The evaluation is done through a comparative between the bio-ethanol consumption of the FCHV, the ideal case and the pure fuel cell case without supercacitors (FC). The ideal case is a reference scenario where the fuel cell always operates in the point of maximum efficiency. The negative percentages in the graph represent the savings of bio-ethanol compared to the pure fuel cell case.

It is remarkable that for the pure fuel cell case, the peak load power required can not be supplied by the fuel cell in the FCHV case. Thus, in the pure fuel cell case is necessary a large fuel cell, thus increasing the cost and consumption. On the other hand, in all driving cycles, hybridization represents an important fuel economy, consuming significantly less than the pure fuel cell case. In fact, in some of them, the hybrid vehicle consumption is very close to the ideal case.

6. CONCLUSIONS

From the simulated results it is concluded that the proposed FCHV pseudo-dynamic model, that includes the entire power train, from the raw material, bio-ethanol, up to the drive train of the vehi-

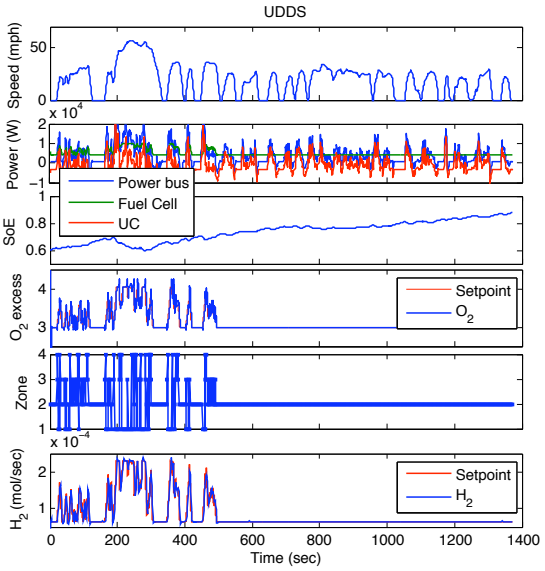

Figure 5: Simulation results for UDDS.

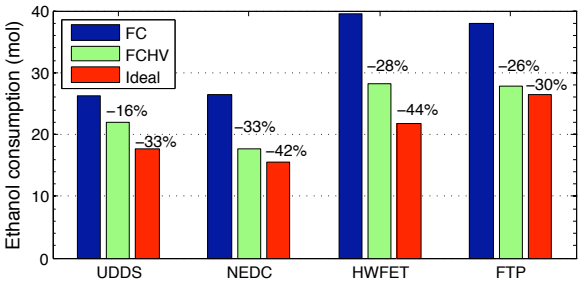

Figure 6: Evaluation of the bio-ethanol consumption for the four driving cycles

cle, is able to support several tests for urban and highway scenarios. Hence, the model helps for developing the conceptual design of a proper energy management strategy. It can be done thanks to the good connection of three different softwares, each of them characterize specific part of the complex real system.

The adequate energy management design, is capable to handle well the required power working inside the good efficiency zones. In addition, the study for two standard driving cycles show that hybridization consumes less bio-ethanol than the FC working alone. The model is used too for plant-wide control structure design.

References

Aicher, T., Full, J. and Schaadt, A., 2009. A portable fuel processor for hydrogen production from ethanol in a 250Wel fuel cell system. International journal of hydrogen energy, 34, 8006-8015.

Aspen Technology Inc. 2006. HYSYS User Manual. Available from: http://www.aspentech.com/hysys/ [Last accessed 2 Jule 2010].

Biset, S., Nieto Degliuomini, L., Basualdo, M., Garcia, V. M., and Serra, M., 2009. Analysis of the Control Structures for an Integrated Ethanol Processor for Proton Exchange Membrane Fuel Cell Systems. *Journal of Power Sources*, 192(1), 107-113.

Chuang, C. C., Chen, Y. H., Ward, J. D., Yu, C. C., Liu, Y. C. and Lee, C. H., 2008. Optimal design of an experimental methanol fuel reformer. *International journal of hydrogen energy*, 33, 7062-7073.

DieselNet, 2010. *Emission Test Cycles*. Available from: http:// www.dieselnet.com / standards / cycles/ [Accessed 29 June 2010].

Feroldi, D., 2009. *Control and design of PEM fuel cell-based systems*. Thesis (PhD).Universitat Politècnica de Catalunya.

Feroldi, D., M. Serra and J. Riera, 2009. Design and analysis of fuel cell hybrid systems oriented to automotive applications, *IEEE Transactions on Vehicular Technology*, 58, 4720-4729.

García, V. M., López, E., Serra, M., Llorca, J., and Riera, J., 2009. Dynamic modeling and controllability analysis of an ethanol reformer for fuel cell application. I*nternational journal of hydrogen energy*, in press, DOI: 10.1016/j.ijhydene.2009.09.064.

Li, X., Xu, L., Hua, J., Lin, X., Li, J. and Ouyang, M., 2009. Power management strategy for vehicular-applied hybrid fuel cell/battery power system. *Journal of Power Sources*, 191(2), 542-549.

Markel, T., Brooker, A., Hendricks, T., Johnson, V., Kelly, K., Kramer, B., O'Keefe, M., Sprik, S., and Wipke, K., 2002. Advisor: a system analysis tool for advanced vehicle modeling. Journal of Power Sources, 110, 255-266.

Nieto Degliuomini, L., Biset, S., Domínguez, J.M. and Basualdo M.S., 2009. Control Oriented Dynamic Rigorous Model of a Fuel Processor System and Fuel Cell Stack. *Computer Aided Chemical Engineering*, 27, 609-614.

Offer, G. J., Howey, D., Contestabile, M., Clague, R. and Brandon, N. P., 2010. Comparative analysis of battery electric, hydrogen fuel cell and hybrid vehicles in a future sustainable road transport system. Energy Policy, 38(1), 24-29.

Pukrushpan, J. T., Stefanopoulou, A. G. and Peng, H., 2004. *Control of Fuel Cell Power Systems: Principles, Modeling, Analysis and Feedback Design*. London: Springer-Verlag.

Thounthong, P., Rael, S., and Davat, B., 2009. Eergy management of fuel cell/battery/supercapacitor hybrid power source for vehicle applications. *Journal of Power Sources*, 193(1), 376-385.

Uzunoglu, M. and Onar, O. and Alam, M., 2007. Dynamic behavior of PEM FCPPs under various load conditions and voltage stability analysis for standalone residential applications. *J. Power Sources*, 168(1), 240-250.